Low temperature dependent ferroelectric resistive switching in epitaxial BiFeO3 films

F. Yan – Harvard University
G. Z. Xing – The University of New South Wales
L. Li –University of Alabama

Citation of published version:

Yan, F., Xing, G., Li, L. (2014): Low temperature dependent ferroelectric resistive switching in epitaxial BiFeO3 films. *Applied Physics Letters*, 104 (13). DOI: 10.1063/1.4870503

Low temperature dependent ferroelectric resistive switching in epitaxial $BiFeO_3$ films

F. Yan, G. Z. Xing, and L. Li

Citation: Appl. Phys. Lett. **104**, 132904 (2014); doi: 10.1063/1.4870503
View online: https://doi.org/10.1063/1.4870503
View Table of Contents: http://aip.scitation.org/toc/apl/104/13
Published by the American Institute of Physics

Low temperature dependent ferroelectric resistive switching in epitaxial $BiFeO_3$ films

F. Yan,[1,a)] G. Z. Xing,[2] and L. Li[3,b)]
[1]*School of Engineering and Applied Sciences, Harvard University, Cambridge, Massachusetts 02138, USA*
[2]*School of Materials Science and Engineering, The University of New South Wales, Sydney, New South Wales 2052, Australia*
[3]*Department of Metallurgical and Materials Engineering, University of Alabama, Tuscaloosa, Alabama 35487, USA*

(Received 2 February 2014; accepted 23 March 2014; published online 2 April 2014)

The ferroelectric switchable diode induced resistive switching behavior at low temperature has been investigated in the epitaxial $BiFeO_3$ (BFO) thin films. The switchable diode can be tuned using a higher voltage at low temperatures. The diode barrier is determined to be ~0.55 eV at the interface between BFO and electrode. The resistive switchable barrier with respect to the ferroelectric domain switching has been systematically characterized at various low temperatures. The temperature dependent conduction and leakage mechanisms have also been identified. These results can advance our understanding of resistive switching based on ferroelectric switchable diode at low working temperatures and potentially extend the applications of memristor to a larger temperature scale. © *2014 AIP Publishing LLC*. [http://dx.doi.org/10.1063/1.4870503]

Next generation information technologies and systems are aimed for higher speed, larger memory density, and significantly enhanced energy efficiency.[1,2] However, current nonvolatile memory technologies, e.g., magnetic random access memory (MRAM) and optical data storage RAM, have approached their technological and physical miniaturization limits.[3,4] An emerging candidate is resistance RAMs (ReRAMs), which are based on resistive switching behavior,[2] featuring with high-speed switching, high-density data storage, and nondestructive readout. Ferroelectric materials are expected to be used as ReRAMs due to the tunable resistivity resultant from the switchable spontaneous polarization.[5] Recently, a tunnel electroresistance effect has been reported, whereby a change in tunneling barrier height is achieved via polarization reversal.[6,7] According to a switchable ferroelectric diode model,[8–10] a Schottky-like barrier can be formed at the interface between a metallic electrode and ferroelectric materials. The switchable diode effect in ferroelectric materials has been attributed to polarization charge[8] in leaky materials or band modification near the ferroelectric/metal interfaces.[11] Till now, most research of ferroelectric resistive switching has been focused primarily at room temperature or above; low temperature study, however, is lacking in the literature. This prohibits the immediate application of this type of memristor at extreme atmosphere, such as space or polar regions.

In this work, we observed the switchable diode effect and ferroelectric resistive switching at low temperatures (100–300 K) in Pt/$BiFeO_3$/$SrRuO_3$ thin film capacitors. The height of the Schottky-like barrier in ferroelectric/metal interface can be tuned by varying the temperature. Our study on the low temperature dependence of the conduction and correlated leakage behaviors involved can provide more details in correlated to the resistive switching behavior, and this work provides valuable details for design and application of the ferroelectric switching based memristors working at low temperature.

Epitaxial $BiFeO_3$ (BFO) films with thickness about 100 nm were grown on single crystalline $SrTiO_3$ (001) substrates with a 50 nm thick epitaxial $SrRuO_3$ (SRO) bottom electrode by pulsed laser deposition, which uses a KrF excimer laser ($\lambda = 248$ nm) with an energy fluence of ~1 J/cm^2 and repetition rate of 3 Hz. The crystalline structure of the BFO films was characterized using X-ray diffractometer (Shimadzu XRD-7000) with a Cu $K\alpha$ radiation. The surface topographies, behaviors of polarization, and nanoscale ferroelectric polarization switching of the BFO films are characterized using a commercial atomic force microscope (AFM) (Asylum Research MFP-3D) with combination techniques of piezoresponse force microscope (PFM) for the local polarization detection. A Pt-coated cantilever (Olympus AC240, nominal spring constant ~ 2 N/m, resonant frequency ~70 kHz) is used with a scanning rate of 0.5 Hz. Pt top electrodes (~20 nm in thickness and ~200 μm in diameter) were sputter-deposited on the films through a shadow mask for electrical testing. The macroscopic current-voltage characteristics and ferroelectric measurements were performed using an electrometer (Keithley 6487) and ferroelectric tester (Radian, US). The temperature dependent investigation was carried out in vacuum (~10^{-5} Torr) on a Lakeshore Cryotronics TTP4 probe station. The film temperature was reduced to 90 K using liquid nitrogen and controlled with a temperature controller (Lake Shore, model 332).

Figure 1(a) shows the X-ray diffraction pattern of the BFO films, confirming that the epitaxial growth of (001) oriented BFO films. The AFM surface image (Fig. 1(b)) indicates that the film surface is smooth with a root-mean-square (RMS) roughness ~1.6 nm. After applying a constant dc bias (9 V) to the conductive tip during the contact-mode scanning, the ferroelectric domain back-switching behaviors are achieved,[9] as shown in Fig. 1(c). The as-grown film prefers an upward

a)fengyan@seas.harvard.edu
b)lin.li@eng.ua.edu

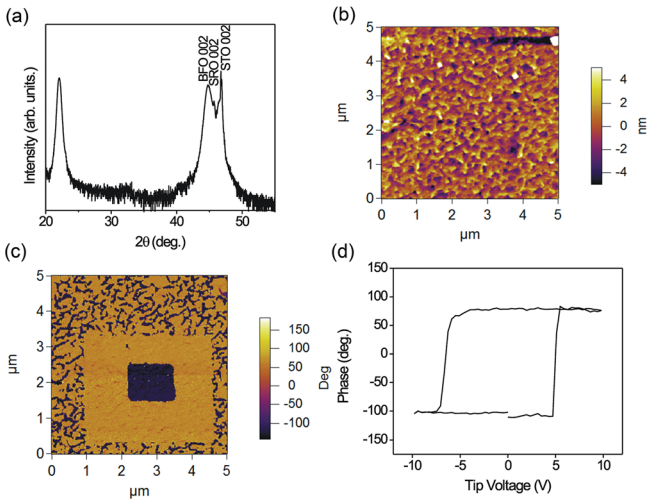

FIG. 1. (a) X-ray diffraction pattern, (b) AFM morphology image, (c) out-of-plane PFM image of a polarization scanned with a tip under ±9 V (outside region corresponds to polarization poled upward under −9 V, and insider region represents downward polarization under +9 V in the as-deposited film), and (d) local PFM phase hysteresis loops for the BFO film, indicating a ferroelectric polarization switching at nanoscale.

polarization and the positive bias voltage switches the ferroelectric polarization downward (+9 V, inside region in Fig. 1(c)). A pronounced hysteresis behavior was obtained using the PFM spectroscopic measurement, as shown in Fig. 1(d), illustrating the ferroelectric polarization switching at nanoscale. Note that the hysteresis loop displays a shift toward a negative voltage due to a self-poling effect caused by the interface barrier between the BFO and SRO bottom electrode.[12,13]

Figure 2(a) shows the *I-V* characteristics measured for the as-grown BFO film at room temperature, and the sequence of voltage is denoted as 1–4. A large switchable diode based ferroelectric resistive switching[8,11] appears. Moreover, the resistive switching behavior can also be obtained by changing the polarization direction of the BFO film. Figs. 2(b) and 2(c) display the corresponding responses of films poled positively (downward polarization) and negatively (upward polarization) under a pulse voltage of 20 V for 100 ms (voltages were both applied on the top Pt electrode), respectively. The current along the downward polarization exhibits a forward diode, whereas the upward polarization induces a reverse diode further confirming that the resistive switching behavior led by the tunable ferroelectric polarization. Figure 2(d) compiles the transport behaviors on a semilogarithmic plot, and the resistive switching (on/off) current ratios are 4, 7, 13 at −4 V for as-grown, downward, and upward polarization, respectively. The resistive switching (on/off) current ratios are lower than the previous results,[8,9,11] which could be contributed to a different film thickness and the existence of interfacial oxygen vacancy defective layer at the film-electrode interface.[11]

The temperature dependence of the current-voltage traces of the BFO film is shown in Fig. 3(a). The high and low resistance states (i.e., HRS and LRS) exhibit a semiconductor behavior and decrease with increasing temperature, indicating that the conduction mechanism is not a filamentary conducting path.[3,14] To assess the effect of temperature on the relationship between the observed switchable resistivity and ferroelectric polarization, we measure the ferroelectric polarization subjected to a fixed sweep voltage range (10 V) at various temperatures (Fig. 3(b)). Below 140 K, the ferroelectric hysteresis loops exhibit pronounced difference in remanent polarization and coercive voltage, which suggests that the ferroelectric domains are more difficult to be switched and thus the corresponding resistivity is greater at lower temperatures. Noted that at a higher temperature (>140 K), the polarization is achieved. Furthermore, the *I-V* responses were measured with increasing scanned voltage at 100 K, as shown in Fig. 3(c). A higher resistivity is observed at lower temperature. The low temperature *I-V* curves are almost symmetric with negligible diode behavior, which suggests that the resistive switching behavior results from the ferroelectric polarization switching in the BFO film. As the temperature increases to 140 K, the switchable diode behavior enhances, as shown in the inset of Fig. 3(a). This

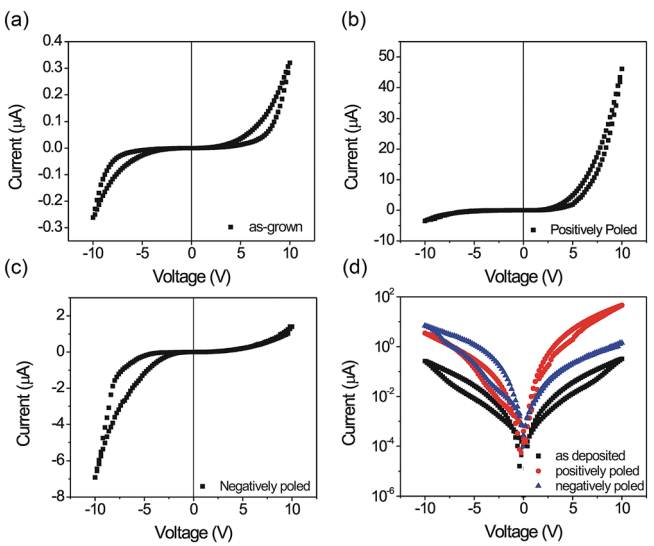

FIG. 2. *I-V* curves for BFO film measured at (a) as-deposited, (b) positively, (c) negatively poled states at room temperature. (d) *I-V* curves plotted on a semilogarithmic scale.

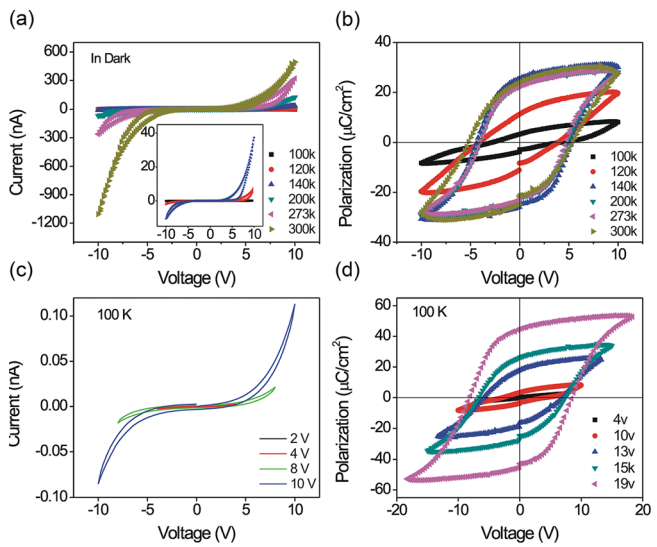

FIG. 3. (a) Resistive switching behaviors and (b) polarization hysteresis loops at various low temperatures measured at 10 V and (c) resistive switching behavior and (d) polarization hysteresis loops upon various voltages measured at 100 K.

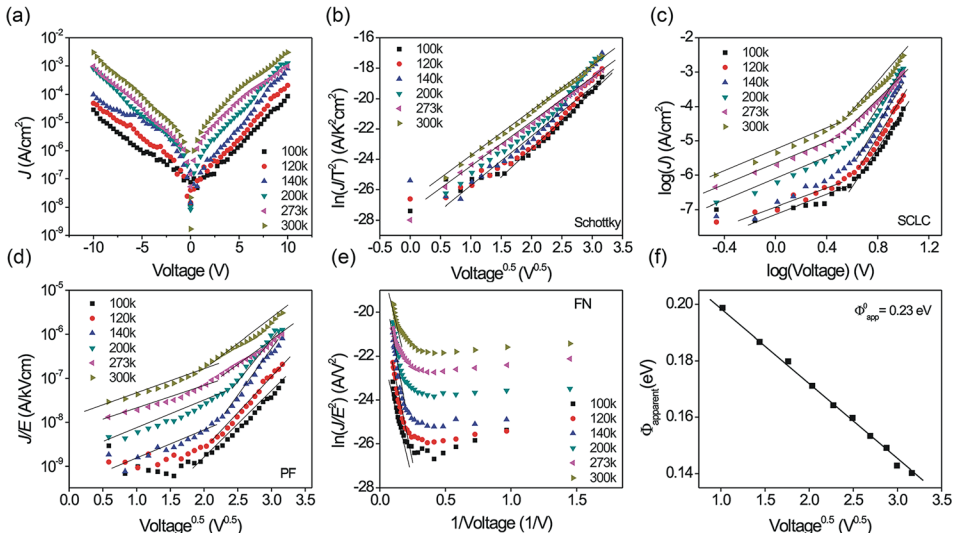

FIG. 4. (a) Typical leakage current density as a function of temperature. Various fits of the leakage current are shown: (b) Schottky emission, (c) SCLC: space charge limits current, (d) PF emission, (e) FN tunneling. (f) Apparent potential barrier versus voltage$^{1/2}$ at room temperature.

indicates that the switchable diode could be driven by the thermal energy and the ferroelectric domain can be switchable. Moreover, the voltage dependence of ferroelectric polarization at 100 K is examined (Fig. 3(d)), where the polarization-voltage hysteresis loops were saturated under 19 V and the remanent polarization was about 50 μC/cm^2. This manifests the ferroelectric nature of our films, i.e., switchable diode behavior, can be triggered using higher electric field at low temperature.

The observed temperature dependent switchable diode effect can be attributed to the polarization-direction dependence of the electrical response at the BFO/electrode interface and the formation of a Schottky-like blocking barrier.[11] We perform the leakage current measurement to further explore the temperature dependent switchable diode induced resistive switching, on the purpose of gaining the underlying mechanisms of the resistive switching. To do so, we first estimate the barrier height at the interface but neglecting the polarization charge.

Figure 4(a) shows the typical leakage current density (*J*-*V* curves) at various temperatures from 100 to 300 K. The *J*-*V* curves elevate with increasing temperature, from 100 to 140 K, and the curves display asymmetric as a consequence of the different work functions of Pt and SRO electrodes,[15] while from 140 to 300 K the *J*-*V* curves become symmetric, indicating a change of underlying leakage mechanisms. The conduction mechanisms can ascribed to interface-limited, Schottky emission[16] (Fig. 4(b)), Fowler Nordheim[17] (FN, Fig. 4(e)) tunneling and bulk limited conduction, Space-charge-limited current[18] (SCLC, Fig. 4(c)), and the Poole-Frenkel (PF, Fig. 4(d)),[16,19] respectively. We have concluded that the dominant leakage mechanisms in our films are temperature dependent, further the striking linear behavior of our data, as shown in Fig. 4(b), strongly supports that the Schottky emission is the dominant mechanism in our measurement, accompanied by slight interface-limited FN tunneling at low temperature (100–140 K) under high voltage (>7 V), as shown in Fig. 4(d).

The Schottky mechanism can be expressed as[20] $J = AT^2 exp - \left[\frac{\Phi_B^0}{k_B T} - \frac{1}{k_B T}\left(\frac{q^3 V}{4\pi\varepsilon_0\varepsilon_{op} d}\right)^{1/2}\right]$, where A is Richardson constant, Φ_B^0 is Schottky potential barrier height at zero applied field, T is the Kelvin temperature, V is the applied voltage, ε_{op} is the optical dielectric constant, and d is the film thickness. The apparent potential barrier[21] is determined by $\Phi_{B,app}^0 = \Phi_B^0 - \sqrt{qP/4\pi\varepsilon_0^2\varepsilon_{op}\varepsilon_{st}}$, where $\Phi_{B,app}^0$ is the apparent potential at zero bias, P is the polarization, and ε_{st} is the static dielectric constant, which is about 54.[22] Thus, the true potential barrier (Φ_B^0) at the BFO/electrode interface at room temperature is calculated to be 0.55 eV according to the Φ_B vs. $V^{1/2}$ relationship (Fig. 4(f)). The barrier height is close to the reported value 0.62 eV, and the difference may be given rise by the defect density in the film.[21] The optical dielectric constant ε_{op} was determined to be about 7.0, and the corresponding optical refractive index n is 2.64 according to $n = \varepsilon_{op}^{1/2}$, which is in agreement with reported n value of about 2.5 from Schottky fitting.[16,23]

To elucidate the conduction mechanisms for the resistive switching at both HRS and LRS, we investigate the ferroelectric polarization charge at the interface.[11] The typical *J*-*V* curves collected at various temperatures are shown in Fig. 5(a). For better illustration, the *J*-*V* curves have also been plotted according to Schottky emission, the SCLC, PF emission, and FN tunneling emission in Figs. 5(b)–5(e). Three features are noted regarding the conduction mechanisms of the BFO films. (i) At 100 K, Schottky emission for LRS with a linear fitting and higher dielectric constant due to the contribution from the interface depletion layer and ferroelectric polarization effect, and PF emission for HRS; (ii) From 120–300 K for the HRS, Schottky emission dominates at lower applied voltage (<7 V) evidenced by the linear relationship of $\ln(J/T^2)$ *vs* $E^{0.5}$, while PF emission plays the key role at higher applied voltage (>7 V) as the calculated optical dielectric constant is in the vicinity of 6.25 (Figs. 5(b) and 5(d)). (iii) At 120–300 K for the LRS, FN tunneling emission at high applied voltage prevails as shown by the negative linear fitting in Figure 5(e). Thereby, we can determine the barrier for the Schottky-like switchable diode for positive and negative bias voltage, as shown in Fig. 5(f), where the positive barrier energy is higher than that of the negative one and varies with temperature.

In summary, we systematically characterized the low temperature switchable diode effect induced resistive switching in the epitaxial BFO films. Combining the analysis of leakage mechanisms at film/electrode interface and the

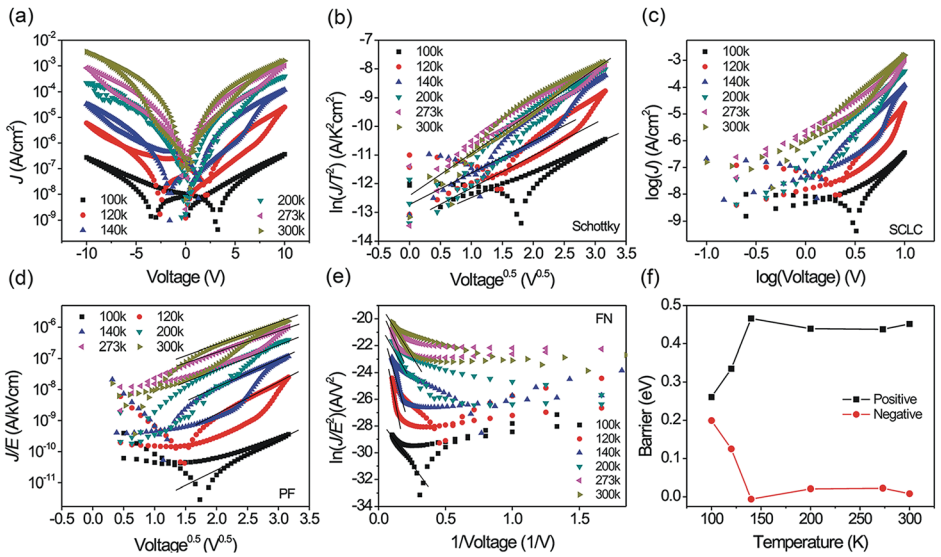

FIG. 5. (a) Typical current-voltage (J-V) curves as a function of temperature in semilogarithmic plots. Various fits of the current mechanisms are shown: (b) Schottky emission at the HRS for lower voltage (<6 V) and higher temperature (>100 K). At 100 K, Schottky emission can be linearly fitted for LRS. (c) SCLC: space charge limits current, (d) PF emission at HRS for higher voltage (>6 V), and (e) FN tunneling for HRS at higher voltage (>6 V). (f) Barrier height as a function of temperature for positive and negative poling process.

current induced barrier height, the Schottky-like barriers for both positive and negative polarized states are determined. The switchable diode relies on temperature and the ferroelectric switchable diode can be manipulated by both the temperature and ferroelectric polarization.

L.L. gratefully acknowledges the financial support from the startup fund at the University of Alabama.

[1]E. Linn, R. Rosezin, C. Kugeler, and R. Waser, Nature Mater. **9**, 403 (2010).
[2]D. B. Strukov and H. Kohlstedt, MRS Bull. **37**, 108 (2012).
[3]S. Akihito, Mater. Today **11**(6), 28–36 (2008).
[4]A. Tsurumaki, H. Yamada, and A. Sawa, Adv. Funct. Mater. **22**, 1040 (2012).
[5]D. Pantel, S. Goetze, D. Hesse, and M. Alexe, ACS Nano **5**, 6032 (2011).
[6]A. Gruverman, D. Wu, H. Lu, Y. Wang, H. W. Jang, C. M. Folkman, M. Y. Zhuravlev, D. Felker, M. Rzchowski, C. B. Eom, and E. Y. Tsymbal, Nano Lett. **9**, 3539 (2009).
[7]P. Maksymovych, S. Jesse, P. Yu, R. Ramesh, A. P. Baddorf, and S. V. Kalinin, Science **324**, 1421 (2009).
[8]C. Wang, K. J. Jin, Z. T. Xu, L. Wang, C. Ge, H.-b. Lu, H. Z. Guo, M. He, and G. Z. Yang, Appl. Phys. Lett. **98**, 192901 (2011).
[9]A. Q. Jiang, C. Wang, K. J. Jin, X. B. Liu, J. F. Scott, C. S. Hwang, T. A. Tang, H. B. Lu, and G. Z. Yang, Adv. Mater. **23**, 1277 (2011).
[10]T. Choi, S. Lee, Y. J. Choi, V. Kiryukhin, and S.-W. Cheong, Science **324**, 63 (2009).
[11]D. Lee, S. H. Baek, T. H. Kim, J. G. Yoon, C. M. Folkman, C. B. Eom, and T. W. Noh, Phys. Rev. B **84**, 125305 (2011).
[12]Y. H. Chu, T. Zhao, M. P. Cruz, Q. Zhan, P. L. Yang, L. W. Martin, M. Huijben, C. H. Yang, F. Zavaliche, H. Zheng, and R. Ramesh, Appl. Phys. Lett. **90**, 252906 (2007).
[13]T. L. Qu, Y. G. Zhao, D. Xie, J. P. Shi, Q. P. Chen, and T. L. Ren, Appl. Phys. Lett. **98**, 173507 (2011).
[14]Z. Yan, Y. Guo, G. Zhang, and J. M. Liu, Adv. Mater. **23**, 1351 (2011).
[15]S. J. Clark and J. Robertson, Appl. Phys. Lett. **90**, 132903 (2007).
[16]G. W. Pabst, L. W. Martin, Y.-H. Chu, and R. Ramesh, Appl. Phys. Lett. **90**, 072902 (2007).
[17]M. A. Khan, T. P. Comyn, and A. J. Bell, Appl. Phys. Lett. **92**, 072908 (2008).
[18]Z. Zhong and H. Ishiwara, Appl. Phys. Lett. **95**, 112902 (2009).
[19]F. Yan, M. O. Lai, L. Lu, and T. J. Zhu, J. Phys. D: Appl. Phys. **44**, 435302 (2011).
[20]L. Pintilie, I. Vrejoiu, D. Hesse, G. LeRhun, and M. Alexe, Phys. Rev. B **75**, 104103 (2007).
[21]L. Pintilie, C. Dragoi, Y. H. Chu, L. W. Martin, R. Ramesh, and M. Alexe, Appl. Phys. Lett. **94**, 232902 (2009).
[22]J. Lu, A. Günther, F. Schrettle, F. Mayr, S. Krohns, P. Lunkenheimer, A. Pimenov, V. D. Travkin, A. A. Mukhin, and A. Loidl, Eur. Phys. J. B **75**, 451 (2010).
[23]C. L. Lu, Y. Wang, L. You, X. Zhou, H. Y. Peng, G. Z. Xing, E. E. M. Chia, C. Panagopoulos, L. Chen, J.-M. Liu, J. Wang, and T. Wu, Appl. Phys. Lett. **97**, 252905 (2010).